Supporting Information

A self-assembled perylene diimide nanobelt for efficient visible-light-driven photocatalytic H_2 evolution

Kangyi Kong[‡a], Shicong Zhang[‡a], Yanmeng Chu[b], Yue Hu[b], Fengtao Yu[a], Haonan Ye[a], Haoran Ding[a] and Jianli Hua[*a]

[a] *Key Laboratory for Advanced Materials and Institute of Fine Chemicals, School of Chemistry and Molecular Engineering, East China University of Science and Technology, 130 Meilong Road, Shanghai 200237, PR China*

[b]*Michael Grätzel Center for Mesoscopic Solar Cells, Wuhan National Laboratory for Optoelectronics, Huazhong University of Science and Technology, Wuhan 430074, Hubei, PR China.*

* Corresponding author. Tel.: +86 21 64250940; fax.: +86 21 64252758.

E-mail address: jlhua@ecust.edu.cn (J. Hua)

Table of Contents

1. Experimental Section

1.1 Preparation of P-PMPDI supramolecular

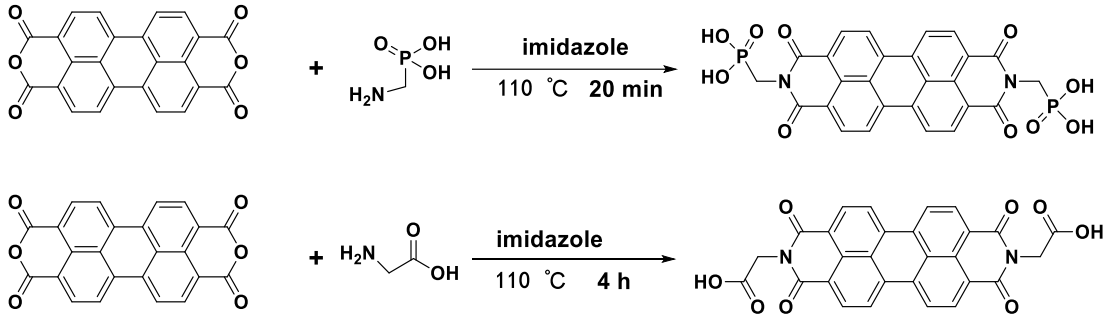

Scheme.S1 Schematic illustration of synthesis of **PDI** molecule

The synthesis of the N, N'-bis(phosphonomethyl)-3,4,9,10-perylenediimide (**PMPDI**) has been carried out by following previous work. [1, 2] Firstly, 790 mg (2.01 mM) 3,4,9,10-Perylenetetracarboxylic dianhydride, 470 mg (2.01 mM) (aminomethyl)phosphonic acid and 15 g imidazole were heated at 130 ℃ for 20 minutes in a three-necked flask. Next 25 mL of 2M HCl and 25mL ethanol were added into the reaction mixture all at once. Solid precipitates would appear immediately and keep these suspensions stirring for another 30 minutes, and then dark solids were collected by centrifugation from above resulting mixture.

Preparation of supramolecular **P-PMPDI**. Above crude product (**PMPDI**) was dispersed in 300 mL deionized water, and it would dissolve in water by dropping 1M NaOH solution into mixture, and then filtrate was collected by centrifugation. After that precipitating the filtrate by adding 2M HCl solution until pH = 1 thus supramolecular **P-PMPDI** formed, and finally collecting the dark solid by centrifugation to separate it from imidazole dissolved in the acidic solution. The collected solid was dried in oven at 50 ℃ overnight for further application.

1.2 Preparation of P-CMPDI supramolecular

The synthesis of the N, N'-bis(carboxylmethyl)-3,4,9,10-perylenediimide (**CMPDI**) refers to previous work. [3, 4] First, 392 mg (1.0 mM) 3,4,9,10-Perylenetetracarboxylic

dianhydride, 675 mg (9.0 mM) Glycine and 7.4 g imidazole were heated under the protection of argon at 110 ℃ for 4h in a three-necked flask. Next 100 mL of 2M HCl and 33 mL ethanol were added into the reaction mixture all at once. Solid precipitates would appear immediately and keep these suspensions stirring overnight, and then dark red solids were collected by centrifugation from above resulting mixture.

Preparation of supramolecular **P-CMPDI**. Above crude product (**CMPDI**) was dispersed in 300 ml deionized water, and it would dissolve in water by dropping 1M NaOH solution into mixture, and then filtrate was collected by centrifugation. After that precipitating the filtrate by adding 2M HCl solution until pH=1, and finally collecting the dark red solid by centrifugation to separate it from the acidic solution. The collected solid was dried in oven at 50 ℃ overnight for further application.

1.3 Pt loaded

Calculated amount of H_2PtCl_6 was added into the 50 mg supramolecular photocatalyst dispersed in 50 mL aqueous solution, and then irradiated by a 300 W Xe-lamp (CEL-HXF300F3, Beijing ceaulight, China) for 5 hours.

2. Testing Section

2.1 Instruments

A Brücker AM 400 spectrometer was employed to obtain ^{1}H NMR spectra with TMS as the internal standard. The crystal structure of the prepared photocatalysts were characterized by using a powder X-ray diffraction (XRD) system (D/max2550VB/PC, Cu Kα radiation). DRS UV–vis absorption spectra were recorded at room temperature on a Varian Cary 500 spectrophotometer. The FTIR spectra were recorded on NICOLET 380 spectrometer using a standard KBr pellet technique in the frequency range of 4000–400 cm^{-1}. The morphology of the photocatalysts was characterized with a scanning electron microscope (SEM, FE-SEM, GeminiSEM 500). TEM and HRTEM images were taken on a transmission electron microscope (TEM, JEM-2100). AFM images were taken on an atomic force microscope (AFM, Veeco/DI). Raman spectra were measured on the microscopic confocal Raman spectrometer (invia reflex) with an excitation of 514 nm laser light. The Photoluminescence (PL) spectrums were obtained on a Hitachi F-4500 fluorescence spectrophotometer at room temperature with an excitation wavelength of 550 nm.

2.2 Photoelectrochemical Measurement

Cyclic voltammetry (CV) curves were measured by a CHI650E electrochemical workstation in a normal three-electrode cell which using glassy carbon as the working electrode, Pt wire as counter electrode and Ag/AgCl electrode as the reference electrode. The experiments were carried out in THF solutions with 0.1 M tetra-*n*-butylammonium hexafluorophosphate ($TBAPF_6$) as the supporting electrolyte at a scan rate of 0.2 V s^{-1}. The ferrocenium/ferrocene (Fc/Fc+) redox couple was used as an external potential reference. The transient photocurrent responses (I–t) and electrochemical impedance spectra (EIS) of composite photocatalyst samples were investigated on a CHI650E electrochemical workstation with a three-electrode (Pt wire, Pt plate, and Ag/AgCl as working, counter, and reference electrode, respectively) system. An aqueous solution of 0.1 M tetra-*n*-butylammonium hexafluorophosphate

($TBAPF_6$) was used as the supporting electrolyte and a 300 W Xe-lamp served as the light source. The films electrodes were prepared as follows:

25 mg of the as-synthesized photocatalysts (**P-PMPDI** and **P-CMPDI**) was separately ground with 10 μL of a Nafon (5%) aqueous solution and 50 μL of ethanol to make slurry. The slurry was then coated onto ITO glass electrodes with an active area of 0.25 cm^2, and these electrolytes were dried at 120 °C for 1 h to evaporate the solvent in muffle furnace. The photocurrent intensity of as-prepared electrodes was measured at 0.3 V versus Ag/AgCl with the light on and off. EIS was determined over the frequency range of 10^2–10^6 Hz with an ac amplitude of 10 mV at the open circuit voltage under room-light illumination.

2.3 Photocatalytic Experiments

The photocatalytic H_2 generation experiments were conducted in a glass gas-closed-circulation system (CEL-SPH2N) under irradiation with a 300 W xenon lamp (CEL-HXF 300). Normally, 50 mg photocatalyst was dispersed in 50 mL (containing 5 mg ascorbic acid (AA)) aqueous. Then sealed with rubber diaphragm air. Before light irradiation, the dissolved air must be thoroughly removed by vacuum pump. And then the aqueous suspension was irradiated from the top using a 300 W xenon lamp jointing a cutoff filter to obtain visible-light irradiation (400 nm < λ< 780 nm). The reaction mixture was kept under constant stirring using a magnetic stirring bar during irradiation and the amount of H_2 gas was detected with the gas phase were determined by an online gas chromatograph (GC 2060, TCD detector, and Ar carrier). In addition, a 300 W xenon lamp with monochromatic light (λ = 380, 420, 500, 550, 630, 700 nm) and 10% dimmer was used as the light source to perform the experiments related to apparent quantum yield.

3. Atomic force micrograph (AFM) of supramolecular

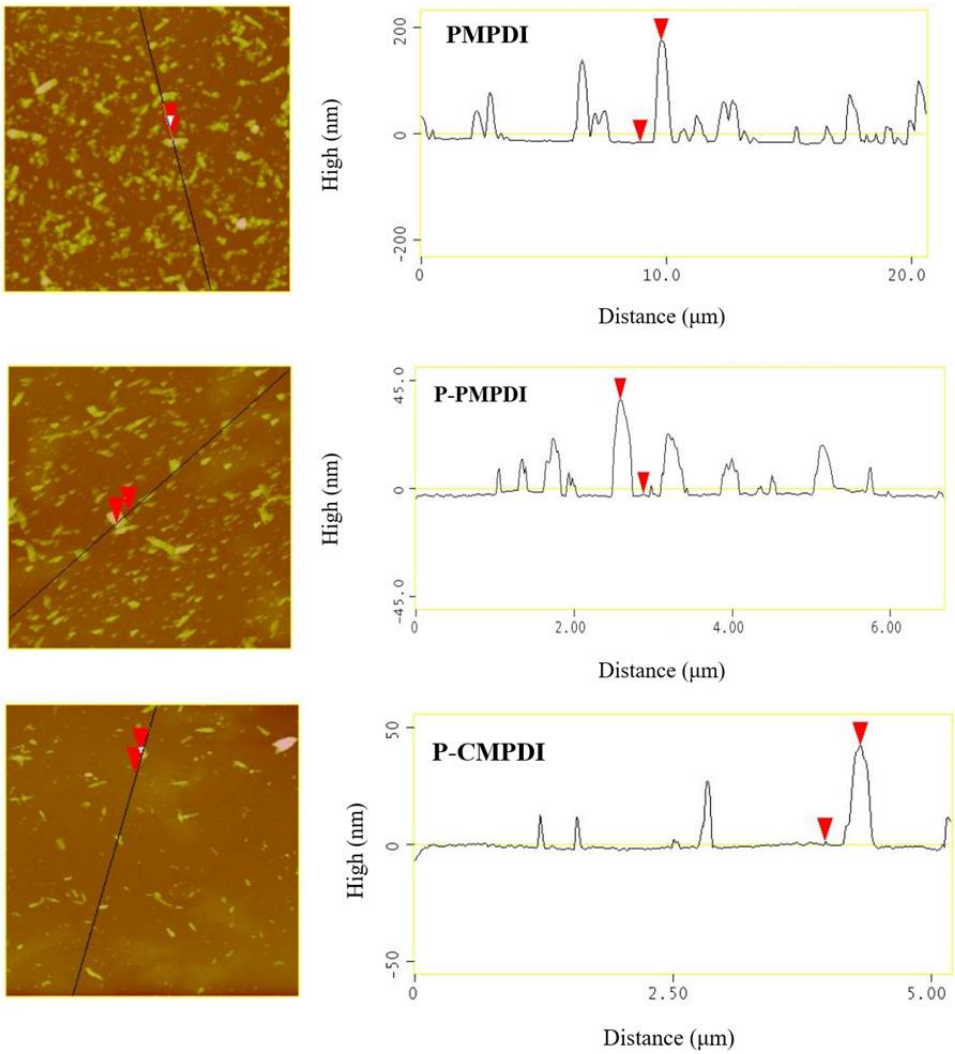

Fig S1. Atomic force micrograph (AFM) of **PMPDI**, **P-PMPDI** and **P-CMPDI**.

4. Proton NMR image of P-PMPDI

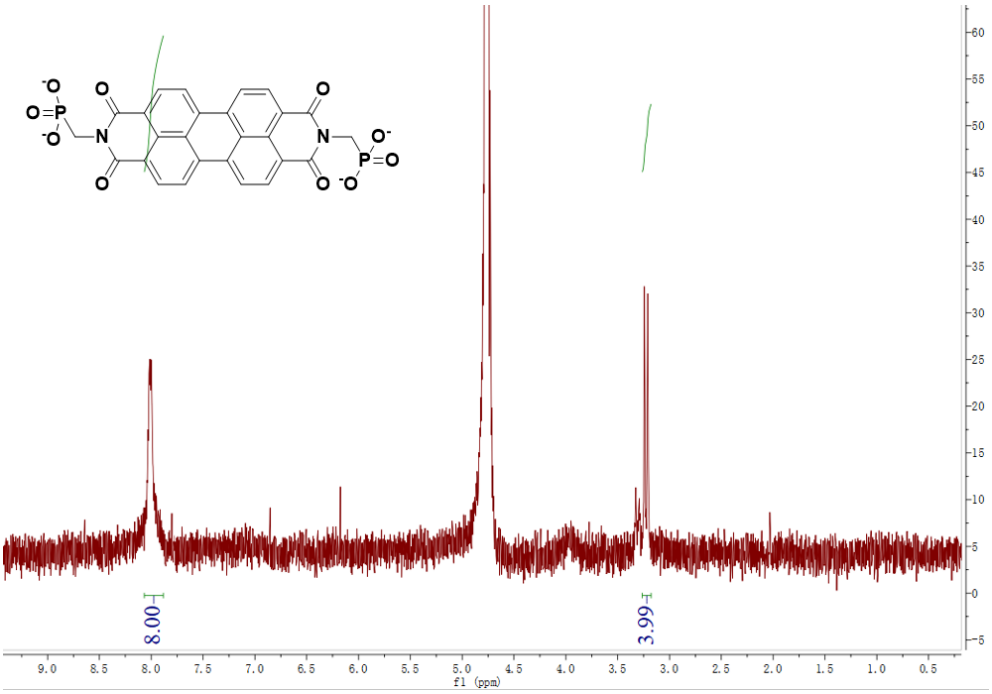

Fig. S2 Proton NMR image of **P-PMPDI** (D2O, wet 1D NaOD solvent suppression)

5. Fourier transform infrared spectra of supramolecular

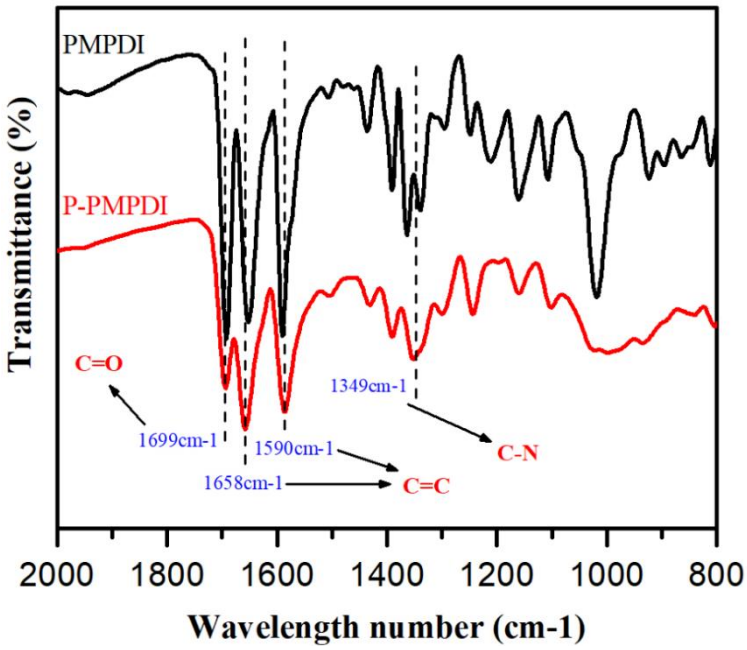

Fig. S3 Fourier transform infrared (FT-IR) spectra of **P-PMPDI** and **PMPDI**

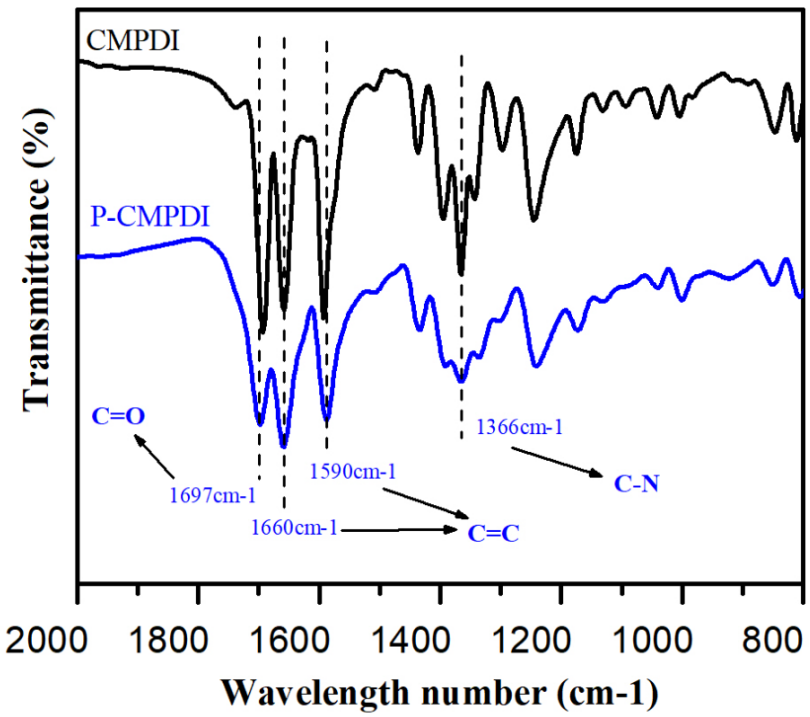

Fig. S4 Fourier transform infrared (FT-IR) spectrum of **P-CMPDI** and **CMPDI**

Table. S1 IR peaks in the **PMPDI, P-PMPDI, CMPDI** and **P-CMPDI**

	C=C stretch	C-N stretch	C=O
PMPDI	1650, 1590 cm^{-1}	1336 cm^{-1}	1691 cm^{-1}
P-PMPDI	1661, 1591 cm^{-1}	1353 cm^{-1}	1699 cm^{-1}
CMPDI	1656, 1590 cm^{-1}	1362 cm^{-1}	1693 cm^{-1}
P-CMPDI	1660, 1590 cm^{-1}	1366 cm^{-1}	1697 cm^{-1}

6. XRD patterns of P-CMPDI

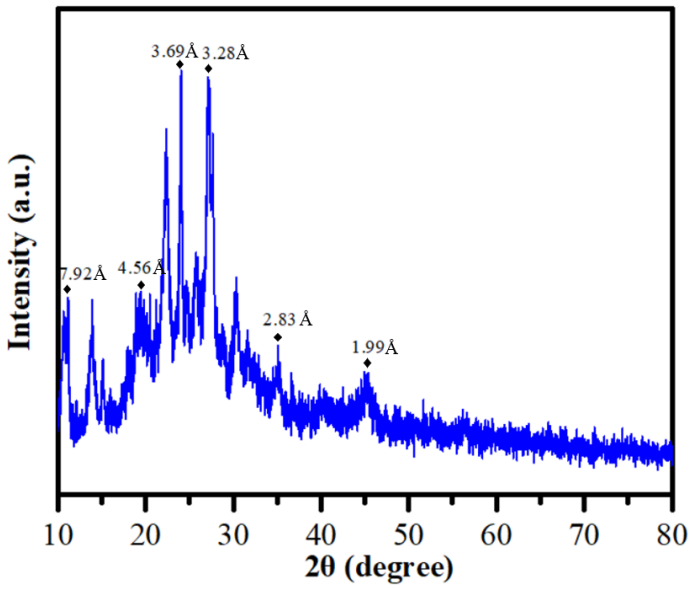

Fig.S5 XRD patterns of **P-CMPDI**

7. Cyclic voltammograms curves of supramolecular and ferrocene/ferrocenium (Fc/Fc+) redox couple

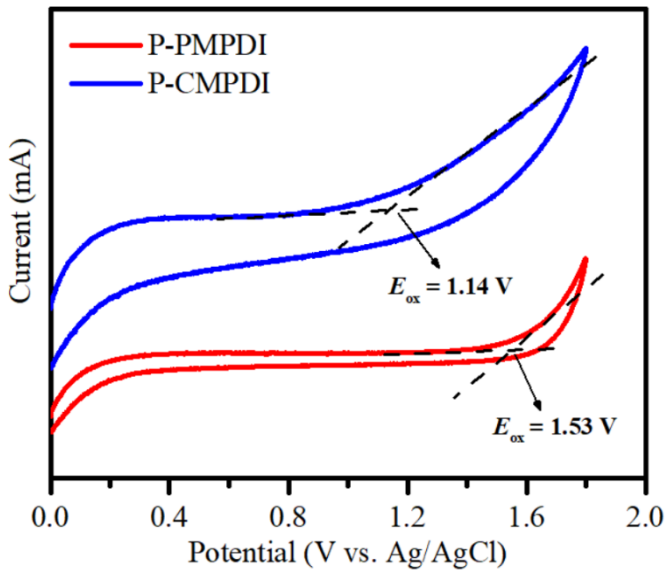

Fig. S6 Cyclic voltammograms curves of **P-PMPDI** and **P-CMPDI**

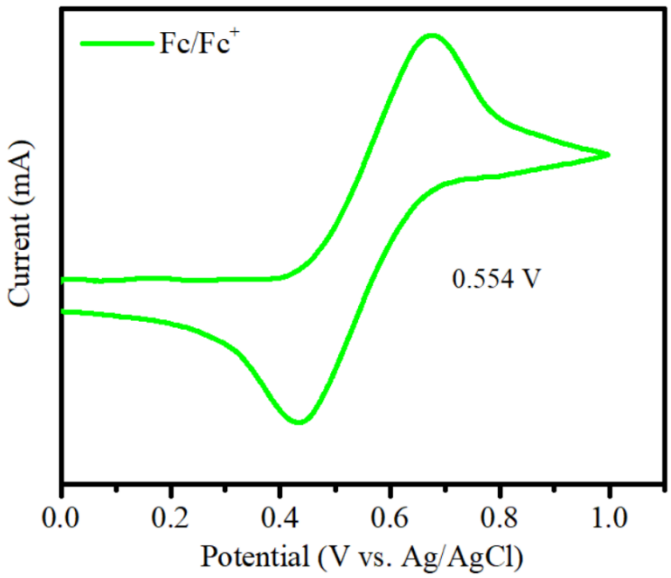

Fig. S7 Cyclic voltammograms curves of ferrocene/ferrocenium (Fc/Fc+) redox couple.

The energy levels of the highest occupied molecular orbital (HOMO) of the self-assembled supramolecular were determined by oxidative half cyclic voltammetry in THF (Fig.S6). Ferrocene/ferrocenium (Fc/Fc^+) was used as an internal reference and 0.1 M tetra-n-butylammonium hexafluorophosphate ($TBAPF_6$) as supporting electrolyte (Fig.S7). The HOMO levels of **P-PMPDI** and **P-CMPDI** were located at 1.28 and 0.89 V vs NHE, respectively, upon the basis of the following relationship[2]

$$-E_{V\ vs.vacuum} = E^{onset} - E_{V\ vs.Fc/Fc^+} + 4.8\ eV$$

$$E_{V\ vs.NHE} = -(E_{V\ vs.vacuum} + 4.5\ eV)$$

The LUMO levels were calculated from the equation of $E_{LUMO} = E_{HOMO} + E_g$ and the associated data were -0.37 V and -0.91 V, respectively, which are higher than the redox potentials of hydrogen evolution, guaranteeing sufficient driving force for water reduction.

8. Molecular orbital distributions in vacuum

Table S2. Molecular orbital distributions and energy optimized in vacuum (isodensity=0.020 a.u.).

	6-31G(d,p)	
	CMPDI	**PMPDI**
LUMO+1	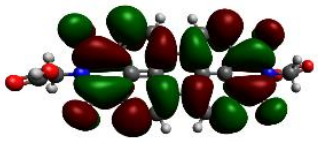 -2.06 eV	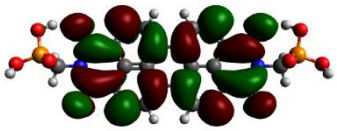 -2.35 eV
LUMO	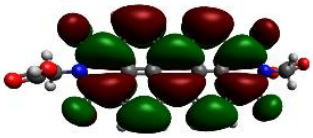 -3.65 eV	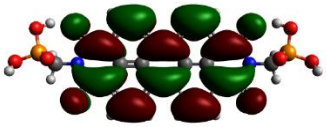 -3.92 eV
HOMO	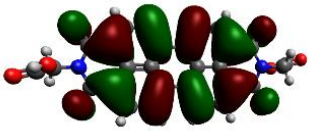 -6.18 eV	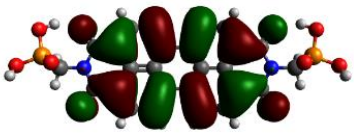 -6.41 eV
HOMO-1	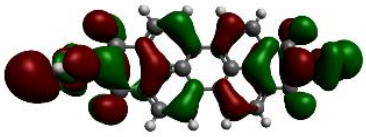 -7.38 eV	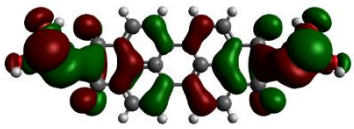 -7.59 eV

Geometry optimizations were carried out on the molecules CMPDI and PMPDI in the gas phase, using the software Avogadro[5] to enter the starting geometry. The molecules were distorted to form a variety of conformers which were then allowed to optimize, in order to find the global minimum on the potential energy surface. Frequency calculations were performed on all the optimized geometries to distinguish whether they were minima or transition states on the potential energy surfaces. Where transition state geometries were found, the bond lengths and angles were distorted in the direction of the vibration and the structure was re-optimized until only positive frequencies were obtained. All calculations were carried out using the Gaussian 09 program[6] with the hybrid B3LYP functional[7] and the standard 6-311G basis set.

9. Calculated apparent quantum yield (AQY) at different wavelengths

$$\text{AQY}\ \ (\%) = \frac{2 \times \text{Number of evolved } H_2 \text{ molecules}}{\text{Number of indicent photons}} \times 100\%$$

$$= \frac{2 \times C \times N_A}{S \times P \times t \times \frac{\lambda}{h \times c}} \times 100\%$$

Where, C is the H2 production amount (μmol) per hour; NA is the Avogadro constant (6.02 × 1023 mol-1); S is the irradiation area (12.56 cm2); P is the monochromatic light intensity (W cm-2) (P is detected by optical power meter); t is the light irradiation time (1h); λ is the wavelength of the monochromatic light (nm); h is the Plank constant (6.626 × 10-34 J s); c is the speed of light (3 × 108 m s-1).

Table S3. Calculated AQY at different wavelengths

Wavelength (nm)	Light intensity (10^{-3} $W\ cm^{-2}$)	[a] Amount of H_2 (μmolh^{-1})	AQY (%)
380	1.85	1.85	1.40
420	1.96	3.18	2.06
500	2.46	3.92	1.67
550	2.41	7.42	2.96
630	2.12	4.80	1.90
700	2.61	0.97	0.26

a. Reaction conditions: 50 mL water, 5 g AA, 50 mg photocatalyst.

λ = 380 nm

$$\text{AQY}\ \ (\%) = \frac{2 \times 1.85 \times 10^{-6} \times 6.02 \times 10^{23}}{12.56 \times 1.85 \times 10^{-3} \times 3600 \times \frac{380 \times 10^{-9}}{6.626 \times 10^{-34} \times 3 \times 10^{8}}} \times 100\% = 1.40\%$$

λ = 420 nm

$$\text{AQY}\ \ (\%) = \frac{2 \times 3.18 \times 10^{-6} \times 6.02 \times 10^{23}}{12.56 \times 1.96 \times 10^{-3} \times 3600 \times \frac{420 \times 10^{-9}}{6.626 \times 10^{-34} \times 3 \times 10^{8}}} \times 100\% = 2.06\%$$

λ = 500 nm

$$\mathrm{AQY}\ (\%) = \frac{2 \times 3.92 \times 10^{-6} \times 6.02 \times 10^{23}}{12.56 \times 2.46 \times 10^{-3} \times 3600 \times \frac{500 \times 10^{-9}}{6.626 \times 10^{-34} \times 3 \times 10^{8}}} \times 100\% = 1.67\%$$

λ = 550 nm

$$\mathrm{AQY}\ (\%) = \frac{2 \times 7.42 \times 10^{-6} \times 6.02 \times 10^{23}}{12.56 \times 2.41 \times 10^{-3} \times 3600 \times \frac{550 \times 10^{-9}}{6.626 \times 10^{-34} \times 3 \times 10^{8}}} \times 100\% = 2.96\%$$

λ = 630 nm

$$\mathrm{AQY}\ (\%) = \frac{2 \times 4.80 \times 10^{-6} \times 6.02 \times 10^{23}}{12.56 \times 2.12 \times 10^{-3} \times 3600 \times \frac{630 \times 10^{-9}}{6.626 \times 10^{-34} \times 3 \times 10^{8}}} \times 100\% = 1.90\%$$

λ = 700 nm

$$\mathrm{AQY}\ (\%) = \frac{2 \times 0.97 \times 10^{-6} \times 6.02 \times 10^{23}}{12.56 \times 2.61 \times 10^{-3} \times 3600 \times \frac{700 \times 10^{-9}}{6.626 \times 10^{-34} \times 3 \times 10^{8}}} \times 100\% = 0.26\%$$

10. Characterization of The recycled catalyst

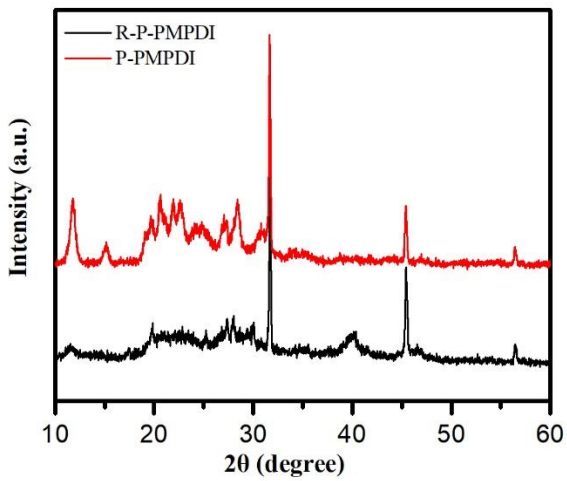

Fig. S8 XRD patterns of **R-P-PMPDI** and **P-PMPDI**

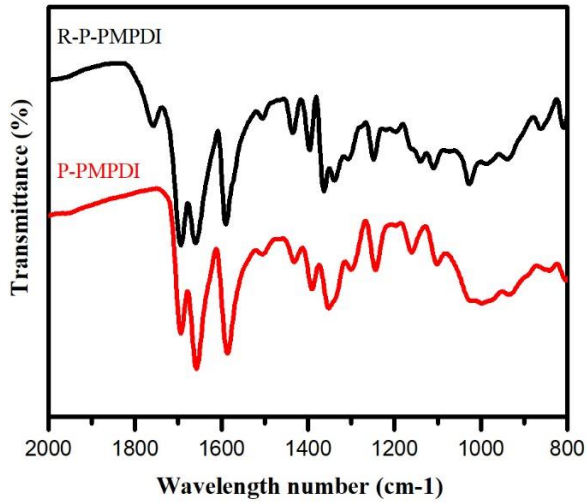

Fig. S9 Fourier transform infrared (FT-IR) spectra of **R-P-PMPDI** and **P-PMPDI**

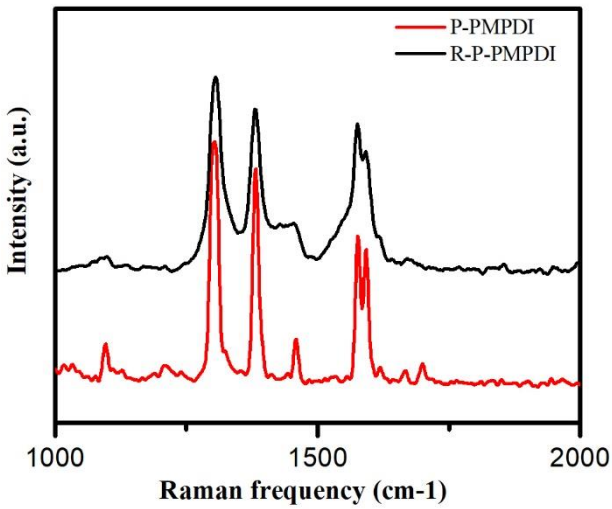

Fig. S10 Raman spectra of **R-P-PMPDI** and **P-PMPDI** powder

11. Photoluminescence spectra of supramolecular

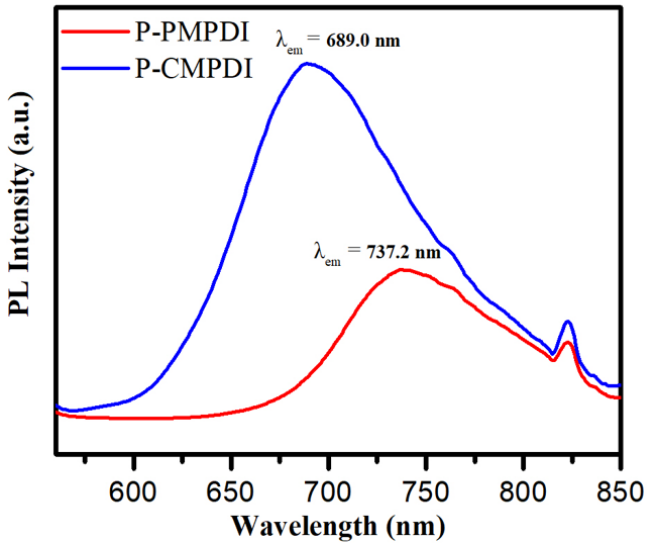

Fig. S11 Photoluminescence (PL) spectra of the **P-PMPDI** and **P-CMPDI**.

12. Photocurrent-time curves on supramolecular membrane electodes

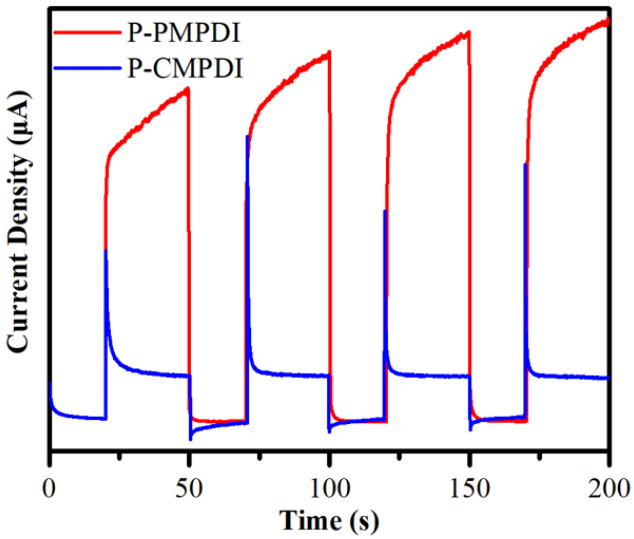

Fig. S12 Photocurrent–time (I–t) curves on **P-PMPDI** and **P-CMPDI** membrane electrodes (0.3 bias).

13. EIS Nyquist plots of supramolecular

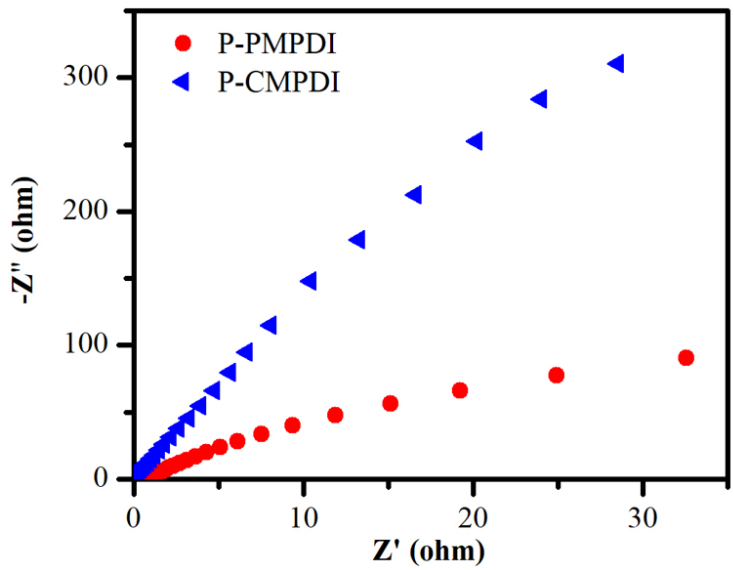

Fig. S13 EIS Nyquist plots of **P-PMPDI** and **P-CMPDI** at open circuit voltage.

14. The reported work previously

Table S4. Comparison of the photocatalytic activity among supramolecular systems.

Photocatalyst	Light Iradiation	Hydrogen Evolution Reaction (HER)	Apparent quantum yield (AQY)	Ref.
PTCDI/Pt/TiO_2	λ ≥ 420 nm	0.075 μmol g^{-1} h^{-1}	0.047% at 550 nm	8
PTCDI-1/Pt/g-C_3N_4	λ ≥ 420 nm	0.375 μmol g^{-1} h^{-1}	0.31% at 420 nm	9
PBI-F/PVP-Pt	λ ≥ 300 nm	0.815 μmol g^{-1} h^{-1}	Not mentioned	10
SA-TCPP-Pt	λ ≥ 420 nm	70 μmol g^{-1} h^{-1}	Not mentioned	11
PorFN-Pt	λ ≥ 420 nm	0.2 mmol g^{-1} h^{-1}	Not mentioned	9
P-PMPDI	λ ≥ 400 nm	11.7 mmol g^{-1} h^{-1}	2.06% at 420 nm 2.96% at 550 nm	This work

15 References

1. B. A. Gregg and M. E. Kose, *Chem. Mater.*, 2008, 20, 5235–5239.
2. J. T. Kirner, J. J. Stracke, B. A. Gregg and R. G. Finke, *ACS Applied Materials & Interfaces*, 2014, **6**, 13367–13377.
3. Hong Miaoa, Jun Yanga, Yunxia Weib, Wenlu Lia and Y. Zhu, *Applied Catalysis B: Environmental*, 2018, **239**, 61–67.
4. Jun Wang, Wen Shi, Di Liu, ZiJian Zhang, Yongfa Zhu and D. Wang, *Applied Catalysis B: Environmenta*l, 2017, **202**, 289–297.
5. M. D. Hanwell et al. J. *Cheminfor*, 2012, **4**, 17.
6. Gaussian 09, Revision A.02, M. J. Frisch, G. W. Trucks, H. B. Schlegel, G. E. Scuseria, M. A. Robb, J. R. Cheeseman, G. Scalmani, V. Barone, B. Mennucci, G. A. Petersson, H. Nakatsuji, M. Caricato, X. Li, H. P. Hratchian, A. F. Izmaylov, J. Bloino, G. Zheng, J. L. Sonnenberg, M. Hada, M. Ehara, K. Toyota, R. Fukuda, J. Hasegawa, M. Ishida, T. Nakajima, Y. Honda, O. Kitao, H. Nakai, T. Vreven, J. A. Montgomery, Jr., J. E. Peralta, F. Ogliaro, M. Bearpark, J. J. Heyd, E. Brothers, K. N. Kudin, V. N. Staroverov, R. Kobayashi, J. Normand, K. Raghavachari, A. Rendell, J. C. Burant, S. S. Iyengar, J. Tomasi, M. Cossi, N. Rega, J. M. Millam, M. Klene, J. E. Knox, J. B. Cross, V. Bakken, C. Adamo, J. Jaramillo, R. Gomperts, R. E. Stratmann, O. Yazyev, A. J. Austin, R. Cammi, C. Pomelli, J. W. Ochterski, R. L. Martin, K. Morokuma, V. G. Zakrzewski, G. A. Voth, P. Salvador, J. J. Dannenberg, S. Dapprich, A. D. Daniels, O. Farkas, J. B. Foresman, J. V. Ortiz, J. Cioslowski, and D. J. Fox, Gaussian, Inc., Wallingford CT, 2009.
7. Becke, A. D. J. *Chem. Phys*. 1993, **98**, 1372–1377.
8. S. Chen, Y. Li and C. Wang, *Rsc. Adv.*, 2015, **5**, 15880–15885.
9. S. Chen, C. Wang, B. R. Bunes, Y. Li, C. Wang and L. Zang, *Applied Catalysis A: General,* 2015, **498**, 63–68.
10. M. C. Nolan, J. J. Walsh, L. L. E. Mears, E. R. Draper, M. Wallace, M. Barrow, B. Dietrich, S. M. King, A. J. Cowan and D. J. Adams, *J. Mater. Chem. A*, 2017, **5**, 7555–7563.
11. Z. Zhang, Y. Zhu, X. Chen, H. Zhang and J. Wang, *Adv Mater*, 2018, **31**,1806626.
12. X. Y. Yang, Z. C. Hu, Q. W. Yin, C. Shu, X. F. Jiang, J. Zhang, X. H. Wang, J. X. Jiang, F. Huang and Y. Cao, *Adv. Funct. Mater.*, 2019, **29**, 1808156.